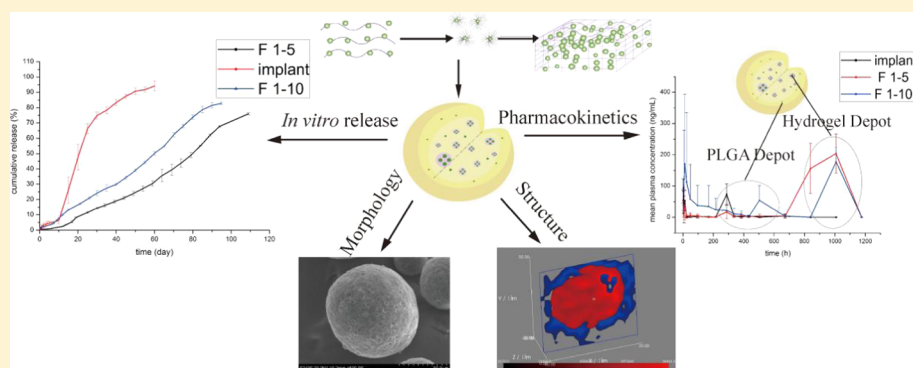# Goserelin Acetate Loaded Poloxamer Hydrogel in PLGA Microspheres: Core−Shell Di-Depot Intramuscular Sustained Release Delivery System

Pan Qi,[†] Ruixuan Bu,[†] Hui Zhang,[†] Jiaojiao Yin,[†] Jin Chen,[†] Anan Zhang,[†] Jingxin Gou,[†] Tian Yin,[‡] Yu Zhang,[†] Haibing He,[†] Puxiu Wang,[§] Xing Tang,[†] and Yanjiao Wang*,[†]

[†]Department of Pharmaceutics, School of Pharmacy and [‡]School of Functional Food and Wine, Shenyang Pharmaceutical University, No. 103 Wenhua Road, Shenyang 110016, China
[§]Department of Pharmacy, The First Affiliated Hospital of China Medical University, Shenyang 110001, Liaoning, China

S *Supporting Information*

ABSTRACT: This study aimed to prepare and optimize goserelin acetate (GOS) loaded hydrogel poly(D,L-lactic acid-*co*-glycolic acid) (PLGA) microsphere that is suitable for long-acting clinical treatment, investigate its structure, and regulate the initial release manner. Here, the PLGA microsphere containing Poloxamer hydrogel loaded with ~15% (w/w) GOS was prepared by double-emulsion−solvent evaporation method and evaluated in terms of microscopic structure, physicochemical properties, and release manner in vitro and in vivo. Raman volume imaging and scanning electron microscopy studies revealed a core−shell Di-Depot structure of the microsphere, in which multi-GOS-loaded hydrogel depots were distributed in the core region. Under the interaction of hydrogel and PLGA depots, high encapsulation efficiency (94.16%) and low burst release (less than 2%) were achieved, along with the accompanying prolonged administration interval (49 days); an enhanced relative bioavailability 9.36-fold higher than that of Zoladex implant was also observed. Also, by addition of 1−5% acetic acid, the lag time was shortened to 6 days. The strategy for regulating the initial release provides new insights for manipulating the release behavior of the PLGA microspheres. The desirable property of the Poloxamer hydrogel PLGA microsphere indicated its promising application in controlled release drug delivery system.

KEYWORDS: goserelin acetate, core−shell structure, lag time, release profile regulation, Di-Depot

1. INTRODUCTION

Goserelin is a small-molecule, highly water-soluble, cationic and acid-stable peptide with good physical and chemical stabilities,[1−3] which could reduce the levels of circulating gonadotrophins (luteinising hormone and follicle-stimulating hormone) and sex hormones during long-term administration.[4] Currently, therapy with a GnRH agonist such as goserelin is considered one of the several first-line options for hormonal therapy in patients with prostate cancer.[5] Goserelin is usually given in its acetate form, which is available as depot preparations. Zoladex, a goserelin acetate (GOS) in situ implant injection, was developed by Astra Zeneca and approved by the FDA in 1996. The GOS long-acting implant is prepared through a hot-melt extrusion method, in which

GOS is dispersed in (D,L)-PLGA (50:50)[2] (Figure 1A). The implant presents as a sterile, white-to-cream colored cylinder with a diameter of 1.0 mm, which is preloaded into a 16-gauge needle for abdominal anterior subcutaneous injection under local anesthesia. This administration usually causes pain and inflammation reactions.[6] Therefore, a different depot preparation that causes limited pain in injection is needed in improving patients' experience.
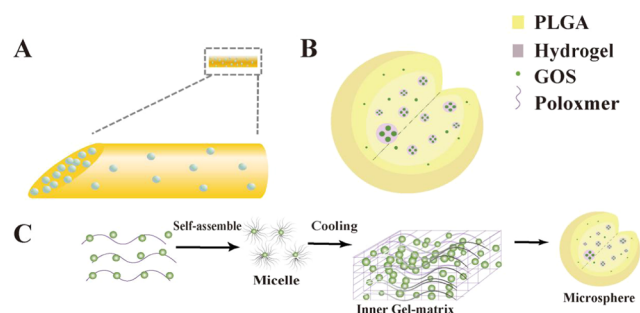
Figure 1. Schematic diagram of the preparations. (A) The solid dispersion structure of the in situ GOS implant. (B) The core−shell structure of GOS Di-Depot microsphere. (C) The formation of GOS-loaded hydrogel poly(D,L-lactic acid-co-glycolic acid) (PLGA) microsphere.

Currently, numerous methods are employed in the preparation of protein/peptide-containing microspheres, such as double-emulsion evaporation (W/O/W), spray drying,[7] electrospray,[8] and ultrasonic atomization,[9] among which the double-emulsion method is the most widely used due to its feasibility.[10] However, it has been reported that the traditional W/O/W method leads to a series of defects such as burst release, low drug-loading (DL) capacity, low encapsulation efficiency, and lag time.[11] Poloxamer has been applied as a hydrogel at the concentration of 15−50% (w/w);[12] with a progressive increase in temperature, Poloxamer micelles rearrange into cubic structure and then into a hexagonal configuration, promoting the gelation process, making Poloxamer hydrogel thermoreversible and thermosensitive. The three-dimensional network structure of Poloxamer hydrogel could not only avoid the harm of hostile environment such as organic solvent or violent shearing during preparation processes but also protect the biological activity and stability of the hydrophilic drug and control the release rate of microsphere during release period.[13−15] F 68 (Poloxamer 188, M_w 7680−9510 Da) and F 127 (Poloxamer 407, M_w 9840−14 600 Da) are employed as hydrogels, among which F 68 enhances the bioadhesive force and has a higher gelation temperature than that of F 127.[16] By introducing Poloxamer hydrogel system into the PLGA microsphere, the viscosity of the inner phase is increased, preventing its leakage significantly; thus, the drug-loading capacity and encapsulation efficiency are increased, while burst release is decreased.[17] Hydrogel PLGA microspheres (Figure 1B) are generally accepted as a delivery system for long periods of drug release with excellent syringeability, which prolong the therapeutic period and reduce the injection pain significantly.[18] In this study, double-emulsion−solvent evaporation method was employed to establish a Di-Depot-controlled release system combining hydrogel with the acid end-capped PLGA biodegradable matrix. The preparation process is shown as Figure 1C: briefly, the Poloxamer and GOS are mixed to form micelles, then assembled to the hydrogel, and finally embedded by the PLGA matrix.

Lag time delays the drug release due to sealed exchange route of peptide drug caused by the formation of a glassy PLGA with reduced PLGA hydrolysis rate and water infiltration.[1,19] It has been reported that the lag time occurring in the microsphere release could be shortened by regulating the pH of the incubating medium.[20] When the PLGA contacts with water, the ester bonds of the PLGA are hydrolyzed to generate acidic oligomers.[21] The acidic degradation products may cause bulk hydrolysis, resulting in the pH value decrease in the surrounding regions and a burst of weight loss at the later stage of the release period,[22] called heterogeneous degradation.[23] Acidic pH as a catalyst is able to accelerate the PLGA hydrolysis and consequently fasten the GOS release, thus regulating the acidity of the inner hydrogel phase would be a feasible way of altering the release manner.

The aim of this study is to prepare a GOS-loaded hydrogel PLGA microsphere, investigate its structure, and modify its release manner. By encapsulating the GOS-loaded hydrogel into the PLGA, microspheres with a core−shell structure were obtained, the encapsulation efficiency was increased, and the burst release was decreased. This is the first time that the pH-regulated hydrogel was employed as the inner phase during the preparation to modify the initial release of the microsphere. The optimized formulation and the strategy of the initial release regulation should provide novel insight for the PLGA microsphere delivery system.

2. MATERIALS AND METHODS

2.1. Material. Carboxyl-terminated PLGA co-polymers (lactide/glycolide molar ratio of 50:50, M_w 30 kDa, i.v. = 0.3 dL/g; M_w 20 kDa, i.v. = 0.24 dL/g; M_w 10 kDa, i.v. = 0.12 dL/g; M_w 1 kDa, i.v. = 0.025 dL/g) were obtained from Jinan Daigang Biomaterials (Shandong, China). GOS (purity > 99.2% determined by HPLC) was obtained from Bachem AG. Poly(vinyl alcohol) (PVA, M_w 30−70 kDa) was obtained from KURARAY Pharmaceutical Co. (Japan). Pluronic F 68 and F 127 were gifts from BASF (Germany). Zoladex implant preparation was obtained from Astra Zeneca. All of the reagents and chemicals used were of analytical or chromatographic grade.

2.2. Preparation of Microspheres. Microspheres were prepared by W/O/W method (Figure S1); briefly, 200 mg of GOS was mixed with 180 mg of F 68 and 20 mg of F 127 in 0.8 mL of water at 4 °C for 10 h to form the hydrogel as the inner phase (W_1). One gram of PLGA polymer dissolved in 4 mL of dichloromethane (DCM) was used as the organic phase (O). In an ice-bath, W_1 and O were emulsified using a high-speed homogenizer at 12 000 rpm (Ultra-Turrax TP 18/10, IKA, Germany) for 2 min to form a primary emulsion. Then, the primary emulsion was injected into 40 mL of 1% PVA solution[24,25] (W_2) and homogenized at 8000 rpm (Ultra-Turrax TP 18/10, IKA, Germany) for 3 min to obtain the double emulsion. Finally, 80 mL of 3% NaAc solution as a diluent was added to the double emulsion, magnetically stirred at 20 °C for 2 h washed with 10 mL of purified water each time for three times, and lyophilized. The final lyophilized microspheres were passed through a 74 μm sieve and subsequently a 37 μm seive to harvest uniform-sized microspheres.[26,27] Formulation variables like molecular weight of the PLGA, the PLGA concentration in the organic phase, the pH of the inner phase, the hydrogel composition, and the solidification method are listed in Table 1.

2.3. Size Distribution Measurement. Microspheres were suspended in distilled water, and the particle size was measured[28] by Dynamic Laser Scattering Analyzer (BT-9300S, Bettersize Co. Ltd., Dandong, China). Each sample was measured in triplicate. The particle size distribution was evaluated by mean particle size (D_{50}) and span value, and the particle size was calculated from the volume distribution using the Mie model. The span value is the measure of the width of

Table 1. Formulation, Encapsulation Efficiency, and Particle Size Distribution of Microspheres[a]

formulation ID	PLGA molecular (kDa)	inner phase composition	inner phase pH (n = 3)	PLGA concentration (mg/mL)	actual DL (%) (n = 3)	EE (%) (n = 3)	mean particle size (μm) (n = 3)	span value (n = 3)
1-1	30	20% hydrogel (F127/F68 = 1:9)	6.71 ± 0.03	250	12.56 ± 0.03	87.90 ± 0.23	72.48 ± 3.89	1.406 ± 0.138
1-2	20	20% hydrogel (F127/F68 = 1:9)	6.71 ± 0.03	250	12.75 ± 0.05	89.32 ± 0.29	64.67 ± 1.72	1.418 ± 0.067
1-3	10	25% hydrogel (F127/F68 = 1:9)	6.74 ± 0.02	150	10.63 ± 0.12	74.53 ± 0.46	54.44 ± 2.43	1.547 ± 0.037
1-4	10	25% hydrogel (F127/F68 = 1:9)	6.74 ± 0.02	200	11.37 ± 0.07	79.64 ± 0.25	59.45 ± 2.57	1.586 ± 0.042
1-5	10	25% hydrogel (F127/F68 = 1:9)	6.74 ± 0.02	250	13.46 ± 0.23	94.16 ± 0.72	67.71 ± 3.08	1.444 ± 0.060
1-6	10	25% hydrogel (F127/F68 = 1:9)	6.74 ± 0.02	250	11.91 ± 0.05	83.42 ± 0.32	58.23 ± 3.52	1.507 ± 0.016
1-7	10:20 kDa = 1:1	25% hydrogel (F127/F68 = 1:9)	6.74 ± 0.02	250	13.14 ± 0.11	92.46 ± 0.61	66.32 ± 2.19	1.448 ± 0.033
1-8	10:1 kDa = 1:1	25% hydrogel (F127/F68 = 1:9)	6.74 ± 0.02	250	11.63 ± 0.23	81.58 ± 1.64	58.11 ± 3.36	1.455 ± 0.059
1-9	10	H₂O	5.64 ± 0.01	250	10.05 ± 0.09	60.36 ± 0.55	70.05 ± 0.43	5.774 ± 0.023
1-10	10	25% hydrogel (F127/F68 = 1:9, 1% HAc)	3.61 ± 0.03	250	12.54 ± 0.09	87.99 ± 0.57	61.58 ± 2.23	1.379 ± 0.064
1-11	10	25% hydrogel (F127/F68 = 1:9, 3% HAc)	2.88 ± 0.03	250	11.41 ± 0.23	79.78 ± 1.66	60.35 ± 3.26	1.477 ± 0.092
1-12	10	25% hydrogel (F127/F68 = 1:9, 5% HAc)	2.74 ± 0.01	250	10.97 ± 0.04	76.85 ± 0.29	65.73 ± 2.85	1.339 ± 0.068
1-13	10	25% hydrogel (F68)	6.82 ± 0.01	250	11.60 ± 0.08	84.04 ± 0.65	65.82 ± 1.24	1.407 ± 0.085
1-14	10	25% hydrogel (F127/F68 = 1:1)	7.03 ± 0.02	250	11.87 ± 0.15	86.06 ± 1.10	63.15 ± 3.26	1.451 ± 0.073
1-15	10	25% hydrogel (F127/F68 = 1:3)	7.07 ± 0.01	250	12.02 ± 0.16	87.14 ± 1.16	64.28 ± 1.58	1.482 ± 0.025
1-16	10	20% hydrogel (F127/F68 = 1:9)	6.71 ± 0.03	250	11.70 ± 0.08	84.90 ± 0.59	52.26 ± 2.06	1.218 ± 0.058
1-17	10	40% hydrogel (F127/F68 = 1:9)	7.12 ± 0.01	250	12.74 ± 0.17	92.17 ± 1.25	79.25 ± 5.73	2.028 ± 0.796

[a](F 1-6 was solidified by rotatory evaporation at 40 °C for 20 min).

the size distribution or the flatness of the distribution curve. For span value <5, the size distribution is considered to be narrow, which is desired.[29] The span value is calculated by the following eq 1.

$$\text{span value} = (D_{90} - D_{10})/D_{50} \tag{1}$$

2.4. Surface Morphology and Structure Observation.

Morphological evolution of the different formulations was monitored by an optical microscope (COIC-500, Chongqing COIC Instrument Co. Ltd., China) and a scanning electron microscope (SEM, S-3400, Hitachi, Japan). The break microspheres were obtained by crushing for the SEM images of inner structure. Atomic force microscopy measurements were performed by an AFM (Cypher ES, Asylum Research) to investigate the detailed information of the microsphere surface. Tetrahedral-tipped silicon-etched cantilevers (AC 240Ts-R3, Oxford Instruments) with a nominal tip radius of curvature of 9 ± 2 nm and a resonant frequency of 3150−6650 kHz were utilized for imaging. Raman volume images were recorded to measure the microsphere structure by a Raman microscope (Renishaw in Via reflex, U.K.) with a Neon laser at wavelength of 633 nm between 3200 and 0 cm^{-1}.

2.5. Powder X-ray Diffraction (PXRD), Differential Scanning Calorimetry (DSC), and Fourier Transform Infrared (FT-IR).

Powder X-ray diffraction (PXRD) patterns were performed with a Cu Kα radiation at a voltage of 40 kV,[10] current of 40 mA, and a scanning rate of 4°/min over a 2θ range from 5 to 60° using a D8 Advance X-ray diffractometer (Bruker, Karlsruhe, Germany). Differential scanning calorimetry (DSC) (DSC-3, METTLER TOLEDO, Switzerland) was used to evaluate the thermodynamic properties of crude GOS and preparations, and the measurement method was as follows, approximately 2−5 mg of the sample was placed in standard aluminum pans, sealed with a lid, and perforated. The samples were scanned at a rate of 10 °C/min over 25 to 200 °C under 50 mL/min flow rate of nitrogen. Fourier transform infrared (FT-IR) spectra of the lyophilized inner phase (200 mg of GOS, 180 mg of F 68, 20 mg of F 127 dissolved in 0.8 mL of H$_2$O and then lyophilized), the physical mixture (200 mg of GOS, 180 mg of F 68, 20 mg of F 127); Poloxamer (mixture of 180 mg of F 68 and 20 mg of F 127), and crude GOS were collected by Fourier transform infrared spectroscopy (Vertex 70, Bruker Optics, Ettlingen, Germany) with a spectral resolution of 4 cm^{-1}. The IR spectra in the wavenumber range of 4000−400 cm^{-1} were recorded for further comparison.

2.6. Loading Efficiency and Encapsulation Efficiency (EE).

The actual drug-loading (actual DL) was measured as follows: 20 mg of microspheres was dissolved in 1 mL of acetonitrile in a 10 mL volumetric flask. One milliliter of glacial acetic acid was added and the mixture was diluted by water to 10 mL. The solution was then centrifuged at 15 000 rpm for 10 min. The supernatant was quantified using ultra performance liquid chromatography (UPLC Acquity, Waters) with a C18 column (ACQUITY BEH C18 2.1 × 50 mm^2, 1.7 μm) and a UV detector (UV wavelength = 220 nm). The column oven temperature was 40 °C, and the mobile phase was 0.5% phosphate in acetonitrile and purity water (25:75, v/v), which was delivered at 0.3 mL/min. The actual drug-loading (actual DL) and theoretical drug-loading (theoretical DL) were calculated using eqs 2 and 3, respectively. The encapsulation efficiency (EE%) was calculated by eq 4.

$$\text{actual DL}(\%) = \frac{W_{\text{GOS in MS}}}{W_{\text{MS}}} \tag{2}$$

$$\text{theoretical DL}(\%) = \frac{W_{\text{GOS}}}{W_{\text{GOS}} + W_{\text{PLGA}} + W_{\text{Poloxamer}}} \tag{3}$$

$$\text{EE}(\%) = \frac{\text{actual DL}}{\text{theoretical DL}} \tag{4}$$

W_{GOS}, $W_{\text{GOS in MS}}$, W_{MS}, $W_{\text{Poloxamer}}$, and W_{PLGA} are the weights of GOS during preparation, GOS in microspheres, microspheres, Poloxamer, and PLGA, respectively.

2.7. Releasing Profiling.

The release medium was 0.01 M phosphate-buffered saline (PBS) buffer (pH 7.4) to mimic the pH and ionic strength of physiological fluids. The in vitro release was measured by suspending 40 mg of microspheres in 2 mL of release medium (pH 7.4) at 37 ± 0.1 °C and shaking at 100 rpm. At each sampling time, the supernatant was totally withdrawn after centrifugation at 3000 rpm for 5 min and replaced by 2 mL of fresh release medium. Each formulation was studied in triplicate. The concentration of GOS in each sample was quantified by UPLC as mentioned in Section 2.6.

2.8. Remaining and Recovery of GOS in Microspheres.

The remaining (%) GOS in microspheres was measured by dissolving the microsphere of F 1-5 and F 1-10 after 50 days of in vitro incubation according to the method introduced under Section 2.6. Recovery (%) of GOS in microspheres was calculated by eq 5. Each samples was detected in triplicate.

$$\text{recovery}(\%) = \text{cumulative release}(\%) + \text{remaining}(\%) \tag{5}$$

GOS purity of F 1-5 and F 1-10 release solution during the 45th to 50th day of incubation was detected by HPLC (UltiMate 2000, Thermo Fisher) with a C18 column (Thermo Hypersil C18, 150 × 4.6 mm^2, 5 μm) and a UV detector (UV wavelength = 220 nm). The column oven temperature was 40 °C, and the mobile phase was 0.5% phosphate in acetonitrile and purity water (25:75, v/v), which was delivered at 1 mL/min. The data were calculated by area normalization method. Each samples was detected in triplicate.

2.9. Ultraviolet and Circular Dichroism (CD) Spectroscopy.

The release solution of F 1-5 and F 1-10 during the 45th to 50th day of incubation and the GOS dissloved in 0.01 M PBS solution were subjected to UV and CD analysis. The UV absorption spectra were recorded on a UV spectrophotometer (UNICO, China, UV-2800A) in the 200−400 nm range. Measurements were performed on 2.5 mL of the sample in quartz cells. CD spectroscopy (Bio-Logic MOS-450, France) experiments were performed in 0.1 and 1 cm quartz cells at the spectral range of 160−400 nm.

2.10. In Vivo Pharmacokinetics Study.

To further investigate the drug absorption in vivo, 15 male Sprague−Dawley rats weighing from 180 to 200 g were randomly divided into three groups (n = 5): group A was given the reference implant by subcutaneous injection as the control group; and groups B and C were given the microspheres of F 1-5 and F 1-10 by an intramuscular injection. The Sprague-Dawley (SD) male rats were housed (each group per cage) and kept under controlled conditions[30] of 12 h light/dark cycle, 22 $\pm$ 2 °C and 50 $\pm$ 15% RH with free access to food and water. All of the procedures were performed according to the guidelines issued by the Ethical Committee of Shenyang

Pharmaceutical University, and the animal study protocol was approved by the University Ethics Committee of Shenyang Pharmaceutical University. The rats were fastened overnight before injection but given access to water throughout the study. Each rat was given the preparation equivalent to 0.9 mg dose of GOS. At predetermined time points, blood samples (approximately 0.5 mL) were taken from the retro-orbital veniplex and collected in heparinized centrifuge tubes. The GOS content in the plasma was then analyzed by a Qtrap 4000 mass spectrometer (Applied Biosystems Sciex, Ontario, Canada). The liquid chromatography–tandem mass spectrometry method was established according to the previous study.[31,32] (The chromatographic separation was performed at 40 °C using a Venusil HILIC column (3 μm, 2.1 × 100 mm^2, Bonna-Agela) with 0.1% formic acid in water (A) and acetonitrile (B) as the mobile phase, which was delivered at 400 μL/min. The gradient was 0–0.01 min of 95% B, 0.01–1.50 min of 95–60% B, 1.50–3.00 min of 60% B, 3.00–3.01 min of 60–95% B, 3.01–6.00 min of 95% B.) The obtained data were analyzed using a noncompartmental method with Drug and Statistics (DAS) software (version 2.0, Mathematical Pharmacology Professional Committee of China, Shanghai, China). The area under a curve (AUC) was calculated[33] according to the trapezoidal rule, and the absorption fraction (*f*) was acquired by eq 6.

$$f = \frac{AUC_{(0-t)}}{AUC_{(0-last)}} \times 100\% \tag{6}$$

2.11. Statistical Analysis. A paired Student's *t*-test was used for the statistical analysis, with $p < 0.05$ considered as the minimum level of significance. Pharmacokinetic parameters were obtained using a noncompartmental method with Drug and Statistics (DAS) software.

3. RESULTS AND DISCUSSION

This research was aimed to prepare a GOS-loaded hydrogel PLGA microsphere, evaluate its morphology, particle size distribution, physical state, structure, and release manner in vitro and in vivo, and provide a strategy of regulating the initial release by changing the pH of the inner phase.

3.1. Selection of Formulation and Preparation Process. Formulation and preparation process are correlated to the properties of the microsphere directly. To obtain the optimized microsphere,[34] several parameters such as the PLGA molecular weight, hydrogel concentration, organic phase concentration, and solidification method were investigated. The formulation used in the process optimization are listed in Table 1 (formulation ID 1-1 to 1-17).

3.1.1. Formulation Selection. To optimize this microsphere-type controlled release system, the hydrogel concentration (F 1-5, F 1-16, and F 1-17) and composition (F 1-5, F 1-13, F 1-14, and F 1-15) of the inner phase and the molecular weights (F 1-1, 1-2, and 1-16) and concentrations (F 1-3, F 1-4, and F 1-5) of the PLGA in the organic phase were investigated for their effect on encapsulation efficiency (Table 1), as well as the cumulative release in vitro (Figure 2).

GOS as a salt[35] decreased the T_{gel} of the Poloxamer hydrogel under 4 °C (Figure S2), so the inner-phase hydrogel was selected mainly due to its effect on the release and EE (%). By comparing 25% (w/w %) hydrogel in different ratios of Poloxamer (F 1-5, F 1-13, F 1-14, and F 1-15), F 127/F 68 = 1:9 (F 1-5) showed a higher EE (%). A decreasing trend in the
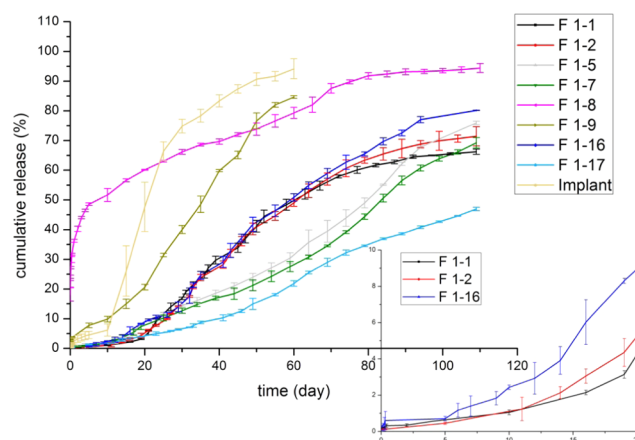

Figure 2. Cumulative release profile of the microspheres prepared with PLGA of different molecular weights (F 1-1, F 1-2, and F 1-16 correspond to PLGA weighing 30, 20, and 10 kDa with 20% hydrogel (F 127/F 68 = 1:9), respectively; F 1-7 and F 1-8 were the PLGA blends (20:10 kDa = 1:1) and PLGA blends (10:1 kDa = 1:1) with 25% hydrogel, respectively; and F 1-5 and F 1-17 were PLGA 10 kDa with 25 and 40% hydrogel (F 127/F 68 = 1:9), respectively. The microspheres were released in vitro for 110 days (*n* = 3). F 1-9 was the microspheres made by PLGA (10 kDa) without Poloxamer hydrogel and Zoladex implant preparation (released for 60 days, *n* = 3).

release rate (Figure S3) was observed with increased hydrogel concentration (F 1-5, F 1-16, and F 1-17). However, F 1-16 (20% hydrogel) showed a lower EE (%) and F 1-17 (40% hydrogel) appeared to have a wider particle size distribution. As a result, 25% hydrogel (F 127/F 68 = 1:9) was finally selected as the inner phase. The EE (%) results (Table 1) showed that the higher concentration of the PLGA in the organic phase resulted in higher viscosity, which prevented the leakage of the inner phase (F 1-3, F 1-4, and F 1-5), thus increasing the encapsulation efficiency.[36] Microspheres prepared with the PLGA of different molecular weights (F 1-1, F 1-2, and F 1-16) showed similar ability to encapsulate GOS-loaded hydrogel, which were uniform in size distribution but slightly different in mean particle size. The cumulative release rate has a negative correlation with the molecular weight (Figures 2 and S4), which could be explained by the characteristic that the molecular weight of the PLGA affects both biodegradation and diffusion,[37] and a longer lag time is usually associated with the higher molecular weight of the PLGA since longer time was required for sufficient bulk erosion to allow drug release.[38] Blends of two different molecular-weight PLGAs also affected the release manner (Figures 2 and S5); microspheres (F 1-8) prepared by PLGA blends (10:1 kDa = 1:1) showed no lag time but instead burst release, while microspheres (F 1-7) prepared by PLGA blends (20:10 kDa = 1:1) showed a slower release rate compared with those (F 1-5) made by PLGA (10 kDa). As a result, F 1-5 was chosen for further research due to their shorter lag time, higher EE (%) as well as negligible burst release compared with other formulations.

Zoladex implant preparation and the microspheres (F 1-9) without adding Poloxamer to the inner phase were used to compare the release manner with the GOS-loaded hydrogel PLGA microsphere (Figure S6). F 1-5, F 1-9, and the implant released 0.66%, 3.66%, and 1.64% of GOS during the first 10 h, respectively. Both F 1-9 and implant showed no obvious lag

time at the initial period and could release for 60 days in vitro. The release profile of F 1-5 showed a lag time of 14 days, and the whole release period was prolonged with a smooth trend, proving its capability in sustained drug release, while the lag time that delayed the release should be regulated.

PLGA microsphere drug-release mechanism could be explained by several theories, such as diffusion through water-filled pores,[39] diffusion through the polymer matrix,[40] osmotic pumping, erosion,[41] and hydrolysis.[42] From the release profile, a diffusion−erosion mechanism based on the Di-Depot interception was hypothesized, which could be divided into three parts: the initial period (Figure 3), stable
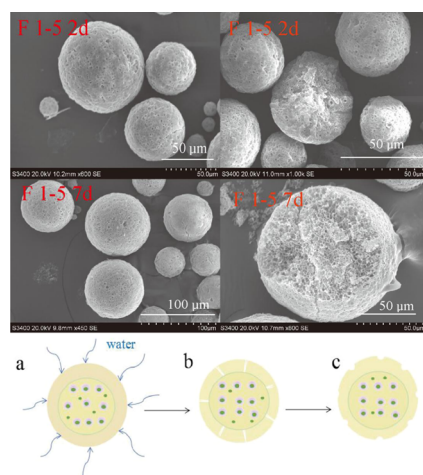

Figure 3. Initial release SEM images of the core−shell Di-Depot microspheres on the surface and in the core region, and the mechanism scheme of the initial release ((a) water uptake; (b) water diffusion into the core region; (c) pores on the shell healed).

period, and final period (Figure 4). During the initial period, water penetrates into the microsphere and diffuses into the inner phase, which causes pore formation.[43,44] Also, as water goes inside the microspheres, the lyophilized inner core is contacted with water and reconstituted as a hydrogel, which turns viscous and blocks the GOS diffusion.[18] Simultaneously, water penetrates into the microsphere with PLGA swelling and the pores in the PLGA shell start healing.[45] Under the interaction of PLGA and hydrogel depots, the GOS release rate is slowed down, called the lag time. The lag time (0−14 days) lasts until the polymer hydrates and loses sufficient mass to initiate the erosion-controlled release.[46] The speculation was supported by the surface pore and inner core (Figure 3) morphology. It was found that during the lag time (F 1-5, 2 and 7 days), the pores on both the surface and internal structure were increased slowly. After the initial period, the pores on the surface increased faster than those in the core region due to the PLGA shell erosion (F 1-5, 15 and 21 days). Therefore, the GOS diffusion from the PLGA depot mainly contributes to the early stage of the stable release period (Figure 4a). In the middle stage of the stable period (F 1-5 30 days), the pores on the shell and core both increased; the GOS-loaded hydrogel depots, which were located in the multicompartment, diffuse from the inner core regions (Figure 4b). Also, in the late stage of the stable period (F 1-5, 50 days), the pores on the inner core became increased, while those on the shell decreased, indicating the pore-closure course, which was caused by the swelling and arrangement of the PLGA
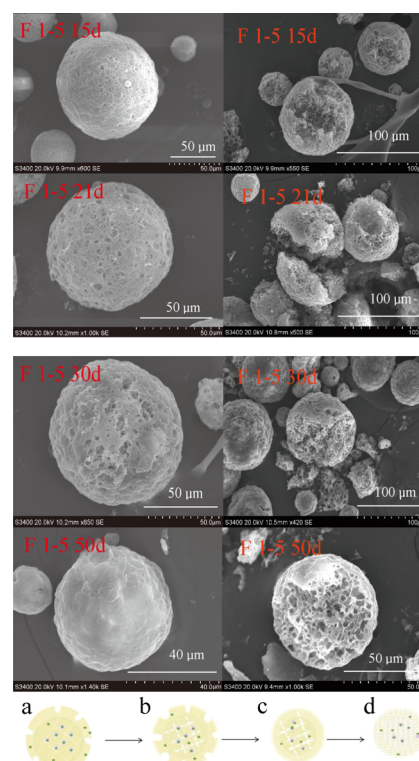

Figure 4. Surface and inner core morphology of the F 1-5 microsphere incubated in release medium (at 15, 21, 30, and 50 days), the mechanism scheme of the stable period and the final period ((a) PLGA shell erosion; (b) inner core PLGA erosion; (c) inner core PLGA erosion, pores on PLGA shell healed; (d) bulk erosion on the shell and core).

chains[47] (Figure 4c). As for the final period, the PLGA degradation was accelerated by acidic PLGA oligomer,[21] thus bulk erosion happened on both shell and core[22] (Figure 4d). It needs to be pointed out that the release profile was formed by the interception of the PLGA depot and hydrogel depot.[18] The Di-Depot structure influences the whole release course and acts differently in controlling the GOS release during the stages.

3.1.2. Shorten Lag Time by Regulating Inner Phase pH. By observing the cumulative release of the GOS-loaded hydrogel PLGA microsphere and Zoladex implant, it seems that the Di-Depot microsphere prolonged the release period significantly. While the lag time of the microsphere is also noticeable, strategies for shortening the lag time should be investigated. In this work, a concentration gradient of acetic acid (F 1-5 and F 1-10 to F 1-12) was employed to investigate the inner phase with different pH values. Upon decreasing the inner phase pH, the encapsulation efficiency decreased (Table 1). This may result from the process when the GOS-loaded hydrogel is homogenized with the organic phase, a certain ratio of hydrogel could not be entrapped by the PLGA−DCM solution, which was removed by contacting with the external phase. GOS has a higher solubility in acetic acid than in water. As the residue increases proportionally, GOS removed by the external phase also increases. From the cumulative release, F 1-10 to F 1-12 showed similar profiles, which were faster than that of F 1-5, and the lag time was shortened from 14 to 6 days (Figure 5). This could be explained by the accelerated hydrolysis of the PLGA shell, which was caused by the incorporated acidic inner phase;[37] thus, the lag time was
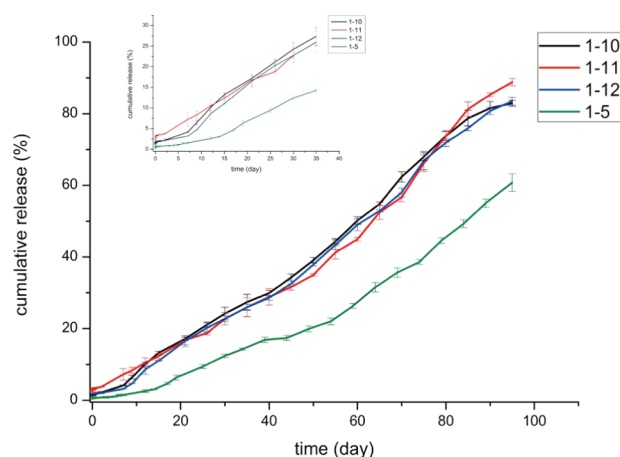
Figure 5. Cumulative release profile of the microspheres (F 1-5 is the microspheres without acetic acid in the inner phase; F 1-10 to F 1-12 are the microspheres adding 1, 3, and 5% acetic acid (w/w %) to the inner phase) incubated in the release medium for 95 days.

shortened by facilitating the PLGA erosion. After lyophilization, acetic acid in the inner phase was removed, leaving an analogous effect on the PLGA matrix, which may explain the phenomenon that the microspheres with different amounts of acetic acid demonstrated similar release profiles. Combining the encapsulation efficiency and release profile, F 1-10 (1% acetic acid) was selected to regulate the initial release. To investigate the effect of acetic acid on the microsphere in vitro, the morphology of the microspheres (F 1-10) incubated in the release medium (2−50 days) at a determined time point was determined by SEM (Figure 6A,B). It seems that there were more pores on the surface of F 1-10 than on F 1-5 during the initial period (Figure 6C); also, the inner core morphology of F 1-10 showed larger pores than F 1-5 after being incubated for 50 days, which indicated that acetic acid would accelerate the degradation behavior of the microsphere.

3.1.3. Effect of Conditions in Solidification Period. It has been reported that increasing the osmotic pressure of the external phase during solvent evaporation could reduce burst release from the PLGA microspheres, as well as improve the release manner.[48] In this work, 3% (w/w) NaAc was employed as a diluent with a higher osmotic pressure. This difference of external phase and the double emulsion in osmotic pressure hindered the mass transfer to the surrounding region;[49] thus, the rate of GOS diffusion outward was decreased. Two DCM removal methods, rotatory evaporation under reduced pressure at 40 °C (F 1-6) and magnetic stirring under atmosphere at 20 °C (F 1-5), were investigated. From the morphology of F 1-5 and F 1-6 (Figure 7), it was indicated that the microspheres solidified by magnetic stirring (F 1-5) had a better surface smoothness than those prepared by rotatory evaporation (F 1-6). Also, the rough surface morphology (Figures 7B and S7B) of the microsphere solidified by rotary evaporation was considered as a consequence of rapid DCM evaporation, which would be responsible for more GOS diffusion out of the inner phase. The encapsulation efficiency of F 1-5 (94.16%) was higher than that of F 1-6 (83.42%), proving more leakage of GOS for the microsphere solidified by rotatory evaporation.

3.2. Characterization of the Microsphere. *3.2.1. Physical State of GOS in the Microsphere.* The physical state of GOS within the microsphere was investigated using DSC (Figure S8A) and PXRD (Figure S8B); the profiles showed
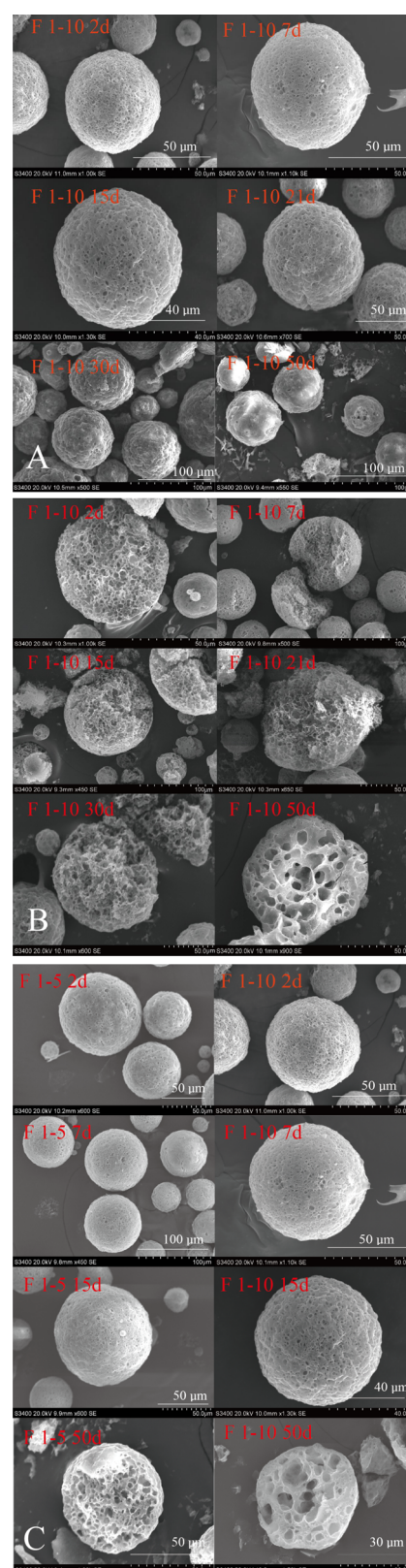

Figure 6. Surface (A) and inner core morphologies (B) of the F 1-10 microspheres incubated in the release medium (2, 7, 15, 21, 30, and 50 days). (C) Surface pores comparison of F 1-5 and F 1-10 during the initial period (2, 7, and 15 days), the inner core morphology comparison of F 1-5 and F 1-10 at 50 days.

that GOS existed in an amorphous state, which was unchanged after encapsulation into the microspheres. The characteristic
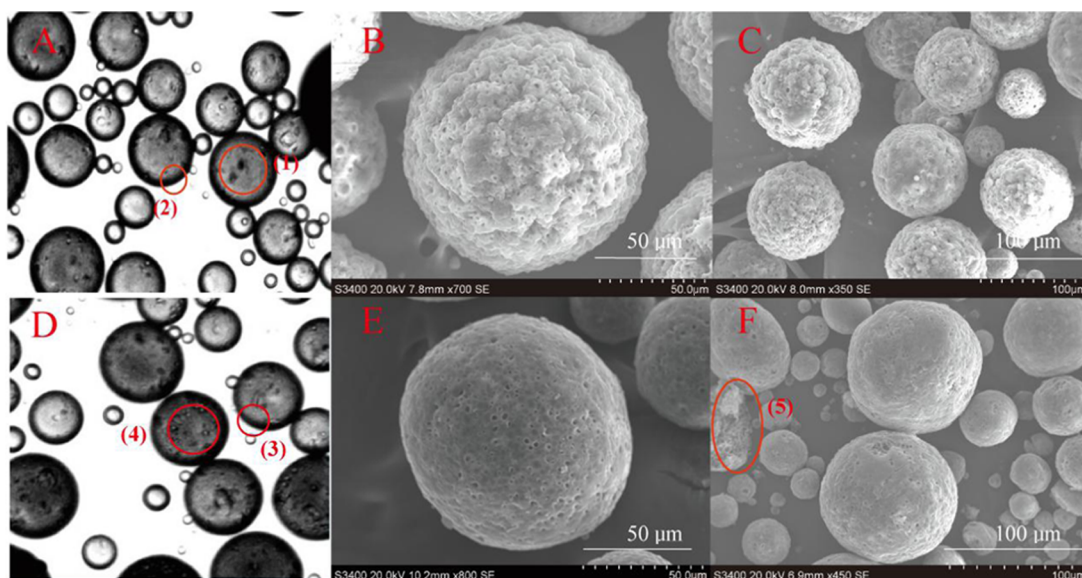
Figure 7. Morphology characterization by optical microscopy ((A) for F 1-6 and (D) for F 1-5) and SEM images ((B) and (C) for F 1-6, (E) and (F) for F 1-5). A(1) and D(4) were the inner core observed in optical microscopy, A(2) and D(3) were the core−shell boundary observed in optical microscopy, and F(5) circled the inner interpenetrating network multicompartment structure in the break microparticle observed in SEM.
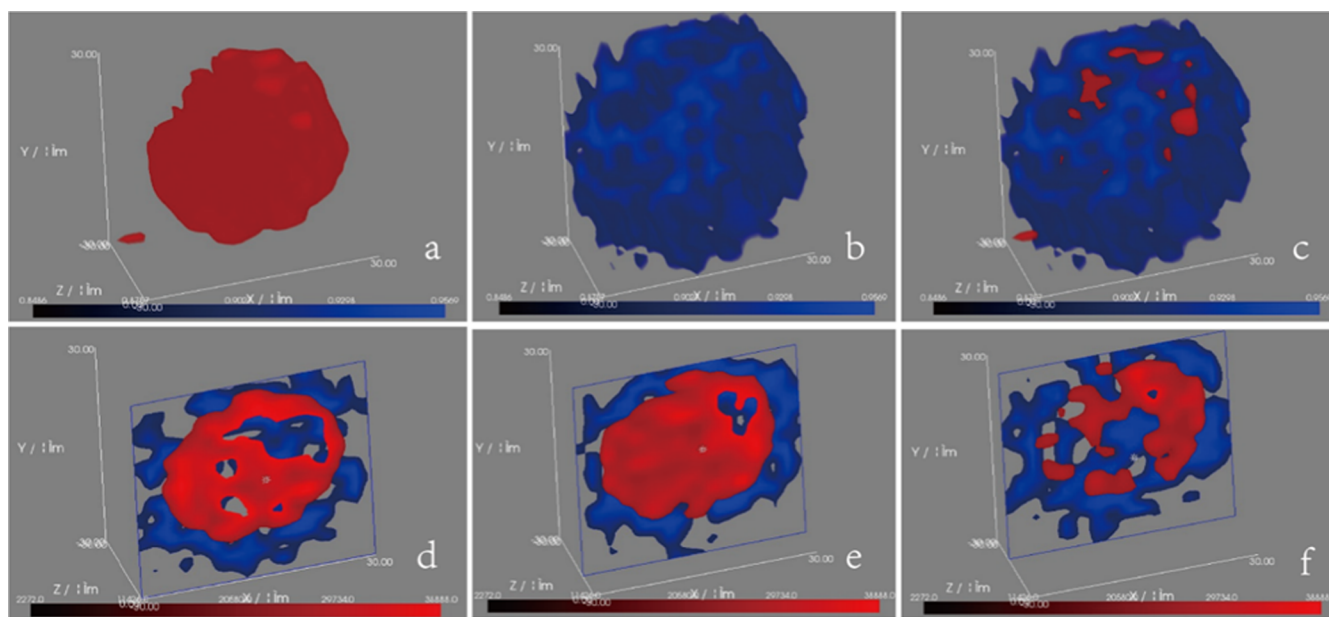

Figure 8. Raman volume image of a microsphere prepared by F 1-5. Red and blue regions were intended for GOS and PLGA, respectively: (a) GOS image; (b) PLGA (10 kDa) image; (c) GOS-loaded hydrogel microsphere image; and (d−f) Raman volume mapping of the microsphere at 0, 10, and 20 μm, respectively.

peaks of Poloxamer in DSC and PXRD decreased a lot in the microspheres, indicating only a little Poloxamer crystalline existed in the microsphere. No shifts in the characteristic peaks of GOS (3280 cm^{-1}) and Poloxamer (2887 cm^{-1}) were observed in the FT-IR spectra (Figure S8E), indicating there was no chemical interaction between GOS and Poloxamer.

3.2.2. Structural Characterization of the Microsphere. To investigate the GOS distribution in the microsphere prepared by F 1-5, Raman spectra (Figure S9) between 3200 and 0 cm^{-1} of GOS and PLGA (10 kDa) were extracted from the chemical maps and typical of the input spectra used to generate images. Raman volume mapping of the GOS-loaded hydrogel PLGA microspheres was performed using Raman shift data between

1827 and 716 cm^{-1}. An interpolated three-dimensional representation of the GOS distribution within a 60 × 60 × 60 μm^3 volume of a microsphere depicting from −30 μm into the microsphere surface (top of image) to 30 μm (bottom of image) of the microsphere bulk (Figure 8) was constructed. The volume images also revealed the core−shell structure of the microsphere, in which the blue boundary showed that the PLGA acted as a shell and GOS and PLGA coexisted in the core region. Blank hydrogel microsphere (without adding GOS), W/O/W microsphere (without adding hydrogel, F 1-9), and GOS-loaded hydrogel microsphere (F 1-5) in two appearances (integral microsphere and break microsphere) were captured by SEM (Figure 9) to compare the morphology.
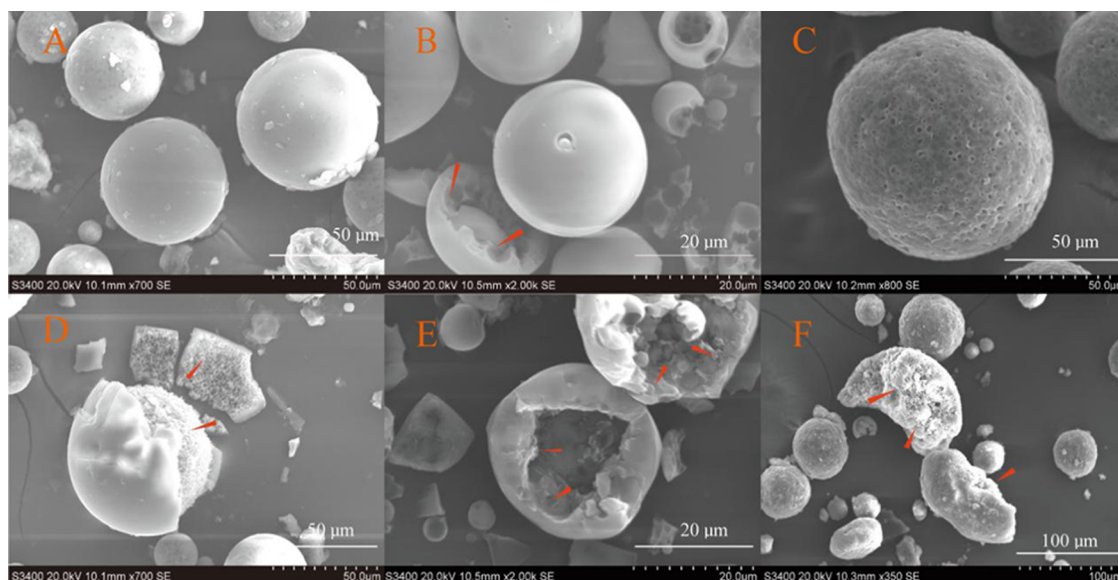
Figure 9. SEM images of the W/O/W microsphere (A, D); blank hydrogel microsphere (B, E); and GOS-loaded hydrogel microsphere (C, F). The inner structure was marked by a red triangle.

Three kinds of microspheres all presented a clear core−shell structure, in which the inner cores had multiple compartments. The W/O/W microsphere and GOS-loaded hydrogel microsphere showed similar honeycomb-like inner structures (Figure 9D,F). While inside the blank hydrogel microspheres, larger compartments were observed, the cavities on the inner wall of the shell also indicated a multicompartment structure of the core (Figure 9B,E).

Combining Raman images with the SEM results, multi-GOS-loaded hydrogel depots embedded by PLGA framework acted as the core, which was assembled with the PLGA shell to form a GOS-loaded hydrogel microsphere. As a result, the hydrogel microsphere delivery system as a Di-Depot was comprised of hydrogel depots and PLGA depots. This Di-Depot microscopic structure might explain the high encapsulation efficiency and prolonged in vitro release.

3.3. Pharmacokinetics and Bioavailability. In this study, the mean plasma concentration−time curve (Figure 10) and the pharmacokinetic parameters (Table 2) of Zoladex implant (group A) administered via subcutaneous injection and GOS-loaded hydrogel PLGA microspheres (groups B and C) administered via intramuscular injection to SD rats are measured to study the release pattern of the hydrogel PLGA microspheres in vivo and find out the effect of acetic acid on the microsphere release manner. Compared with the implant group, both the microsphere groups showed a longer T_{max} and mean retention time (MRT), indicating the microsphere with hydrogel core could achieve a longer release period.[17] C_{max} of the implant occurred at approximately 12th day, and the mean plasma concentration−time profile of the microsphere (F 1-5) showed two peaks, among which the first little peak at the 12th day and the second peak at the 42nd day were mainly caused by GOS dispersed in the PLGA depot in a multihydrogel core,[17] respectively (Figure 10). The two peak plasma concentration profiles enabled the microspheres prepared by F 1-5 and F 1-10 to achieve AUC_{0-t} that is 9.36-fold and 7.52-fold greater than that of the Zoladex implant.[33] The increased relative bioavailability could be ascribed to the higher plasma concentration peak by Poloxamer hydrogel depot.[17] By adding
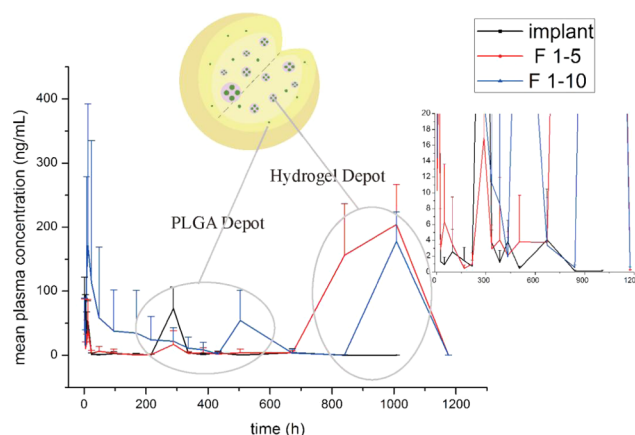

Figure 10. Mean plasma concentration in rats receiving implant (group A), F 1-5 (group B), and F 1-10 (group C); the profile of concentration at 0−20 ng/mL was enlarged. The first peak on 12th day and the second peak on 42nd day were mainly caused by GOS dispersed in the PLGA depot and multihydrogel depots, respectively.

1% acetic acid to the hydrogel core, the two characteristic peaks of the hydrogel PLGA bilayer microsphere remained with the first peak higher and slower (Figure 10). Absorption fraction (Figure 11) of F 1-5 and F 1-10 showed a similar trend with the cumulative release in vitro, proving that the microsphere prolonged the therapeutic effect. By regulating the acidity of the hydrogel core, the microsphere (F 1-10) showed modified release manner and the lag time was shortened, which proved the effect of acetic acid on regulating the initial release.

The PLGA microspheres prepared by the double-emulsion method for peptide or protein delivery system would face the stability problems caused by organic solvent or shearing stress during preparation and the hydrolysis of the PLGA during release, which might destroy the structural integrity of the peptides or proteins.[50] To further evaluate the structural integrity and chemical stability of GOS during release, circular dichroism (CD)[51] and ultraviolet (UV)[52] spectra, GOS purity, and recovery from the microsphere during in vitro release were

Table 2. Pharmacokinetic Evaluation Parameters of GOS in SD rats ($n = 5$)

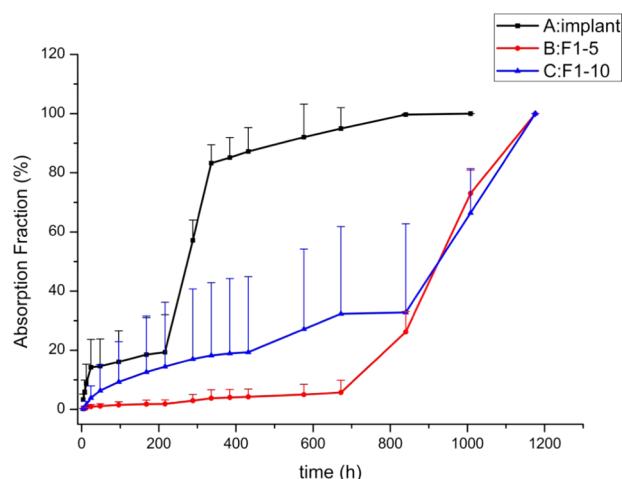| parameters	Zoladex implant	F 1-5	F 1-10
AUC_{0-t} (μg·h/L)	6858.016 ± 1966.210	64 232.309 ± 15 510.585	51 458.977 ± 23 185.522
$AUC_{0-\infty}$ (μg·h/L)	6865.567 ± 1965.128	201 130.680 ± 132 639.320	102 436.700 ± 49 270.503
$MRT_{(0-t)}$ (h)	282.358 ± 70.031	897.153 ± 23.182	771.908 ± 242.625
T_{max} (h)	192.333 ± 165.700	966.000 ± 84.000	759.000 ± 498.000
C_{max} (μg/L)	102.905 ± 25.165	218.019 ± 35.147	267.444 ± 160.015

Figure 11. Absorption fraction in rats receiving implant (group A), microsphere prepared by F 1-5 (group B), and F 1-10 (group C) ($n = 5$).

investigated. Considering the microspheres could release for around 50 days in vivo, the release solution of F 1-5 and F 1-10 during the 45th to 50th day of incubation was employed for analysis. Until the 50th day, the purity of GOS in the release solution was around 94% and the recovery of F 1-5 and F 1-10 were 91.63 and 95.08%, respectively (Table S1), indicating the good chemical stability of GOS during the 50 day of release, which met the requirement of the long-term release. CD (Figure S10) profiles of the GOS solution and the release solution during 45th to 50th day showed no significant difference; the UV absorption spectra (Figure S11) of the release solution indicated the characteristic bands of aromatic peptide side chains,[53] which was also consistent with the spectra of the GOS solution, indicating that the structure of GOS was basically unchanged after 50 days of incubation. From the pharmacokinetics results, the AUC_{0-t} of the microspheres (F 1-5 and F 1-10) were 9.36-fold and 7.52-fold greater than that of the Zoladex implant, proving that GOS delivered by the Di-Depot microsphere achieved a high relative bioavailability. In summary, the structural integrity and chemical stability of GOS were maintained during 50 days of incubation, making it suitable for the Poloxamer hydrogel PLGA microsphere delivery system. Good chemical stability of GOS,[3] fine compatibility of GOS and PLGA,[2] and the protection of Poloxamer hydrogel[14] contribute to the desirable structural integrity during the release.

Current research on GOS focuses on the pharmacological action[54,55] and combined medication[56] of GOS or Zoladex, with only a few studies on GOS in other drug delivery systems. It has been reported that the GOS-loaded poly(ethylene glycol)−polycaprolactone nanoparticles delivery system had a inhibitory effect on the prostatic cell for 3 days.[57] As for long-acting formulations, the Zoladex implant, which is prepared by

hot-melt extrusion method,[58] has a therapeutic efficiency of a month. However, the Zoladex administration is always accompanied by severe pain and bleeding caused by the injection of the implant,[6] which are the main drawbacks. Attempts have been made to solve it by physical means such as cooling the local skin with ice[6] or entrapping GOS into the microspheres to reduce the particle size of the preparation.[25] It has been reported[59] that in the preparation of the GOS microsphere by the S/O/W method, GOS was mixed with poloxamer and poly(ethylene glycol) to form a solid powder mixture by hot-melt or lyophilization and then encapsulated by PLGA (4−30 kDa). The S/O/W GOS microspheres showed 15−28 days of sustained release in vivo. Higher EE (%) (higher than 90%) of the S/O/W microspheres was achieved due to GOS−solid powder mixture embedded in the PLGA matrix and introducing Poloxamer into the microsphere improved the bioavailability (higher than 1.2-fold) compared with that of the W/O/W GOS microspheres. In this work, the GOS-loaded hydrogel microspheres were prepared with good properties: higher EE (%) (higher than 90%), longer release period (49 days in vivo), higher bioavailability (9.36-fold), and smaller particle size. The reduced particle size could relieve the pain during administration compared to Zoladex. Also, the desirable characteristics of the microspheres are correlated to its core−shell structure, which is different form the solid dispersion structure of Zoladex.

4. CONCLUSIONS

In this study, a core−shell structure of the Di-Depot-controlled release system for the GOS-loaded Poloxamer hydrogel PLGA microsphere was established. The optimized formulation (F 1-5) was selected by investigating the composition of the inner phase and organic phase, as well as solidification methods, which overcame common the defects of microspheres prepared by the W/O/W method, resulting in a high encapsulation efficiency and a long release period with good stability. A clear core−shell structure was observed by Raman volume image, which determined the sustained release manner in vitro, a prolonged dosing cycle, and a higher $AUC_{0-\infty}$ compared to those of Zoladex in vivo. The hydrogel and the PLGA assembled Di-Depot for GOS delivery, resulting in a double-peak plasma concentration pattern, in which GOS dispersed in the PLGA depot diffused in early stage to form the first peak at the 12th day and GOS concentrated in Poloxamer hydrogel depots diffused successively in the later stage to form the second peak at the 42nd day. However, a lag time that delayed the drug release was also observed. By reducing the pH of the inner phase, a heterogeneous degradation was triggered by acetic acid. As a result, the lag time in vitro was shortened from 14 to 6 days, and the in vivo absorption fraction also showed an accelerated release with a stable pattern. The GOS-loaded Poloxamer hydrogel PLGA microspheres could reduce the dosing size and relieve the pain caused by the Zoladex implant, which is promising in controlled release system and suitable for

application with the acetate salts of another GnRHa with similar physical−chemical properties such as those of triptorin and leuprolide.

ASSOCIATED CONTENT

Ⓢ Supporting Information

The Supporting Information is available free of charge on the ACS Publications website at DOI: 10.1021/acs.molpharmaceut.9b00344.

> Manufacturing process, T_{gel} decrease by GOS, effect of hydrogel concentration, effect of PLGA molecular weight, effect of PLGA blends, comparison with reference, AFM images, physical state characterization, and Raman spectra of GOS and PLGA (PDF)

AUTHOR INFORMATION

Corresponding Author

*E-mail: tanglab@126.com. Tel: 86-24-23986343. Fax: 86-24-23911736.

ORCID Ⓘ

Yanjiao Wang: 0000-0001-5313-9901

Notes

The authors declare no competing financial interest.

ACKNOWLEDGMENTS

ABBREVIATIONS

PLGA, poly(D,L-lactic acid-*co*-glycolic acid); DCM, dichloromethane; PVA, poly(vinyl alcohol); F68, Poloxamer 188; F127, Poloxamer 407; NaAc, sodium acetate; D_{50}, mean particle size; EE, encapsulation efficiency; SEM, scanning electron microscopy; AFM, atomic force microscopy

REFERENCES

(1) Hirota, K.; Doty, A. C.; Ackermann, R.; et al. Characterizing release mechanisms of leuprolide acetate-loaded PLGA microspheres for IVIVC development I: In vitro evaluation. *J. Controlled Release* **2016**, *244*, 302−313.

(2) Camble, R.; Timms, D.; James, W. A. Continuous release pharmaceutical compositions. U.S. Patent US5320840, 1994.

(3) Wang, J.; Yadav, V.; Smart, A. L.; et al. Toward Oral Delivery of Biopharmaceuticals: An Assessment of the Gastrointestinal Stability of 17 Peptide Drugs. *Mol. Pharmaceutics* **2015**, *12*, 966−973.

(4) Brogden, R. N.; Faulds, D. Goserelin. A review of its pharmacodynamic and pharmacokinetic properties and therapeutic efficacy in prostate cancer. *Drugs Aging* **1995**, *6*, 324−343.

(5) Cheer, S. M.; Plosker, G. L.; Simpson, D.; et al. Goserelin: a review of its use in the treatment of early breast cancer in premenopausal and perimenopausal women. *Drugs* **2005**, *65*, 2639.

(6) Kinoshita, H.; Kawa, G.; Hiura, Y.; et al. Effectiveness of skin icing in reducing pain associated with goserelin acetate injection. *Int. J. Clin. Oncol.* **2010**, *15*, 472−475.

(7) Yang, Y.; Chen, Q.; Lin, J.; et al. Recent advance in polymer based microspheric systems for controlled protein and peptide delivery. *Curr. Med. Chem.* **2019**, DOI: 10.2174/0929867326666190409130207.

(8) Zhao, Q.; Wang, M. Manipulating the release of growth factors from biodegradable microspheres for potentially different therapeutic effects by using two different electrospray techniques for microsphere fabrication. *Polym. Degrad. Stab.* **2019**, *162*, 169−179.

(9) Ye, M.; Kim, S.; Park, K. Issues in long-term protein delivery using biodegradable microparticles. *J. Controlled Release* **2010**, *146*, 241−260.

(10) Guo, Y.; Yang, Y.; He, L.; et al. Injectable Sustained-Release Depots of PLGA Microspheres for Insoluble Drugs Prepared by Hot-Melt Extrusion. *Pharm. Res.* **2017**, *34*, 2211−2222.

(11) Shi, Y.; Ma, S.; Tian, R.; et al. Manufacture, Characterization and Release Profiles of Insulin-Loaded Mesoporous PLGA Microspheres. *Mater. Manuf. Processes* **2016**, *31*, 1061−1065.

(12) Rowe, R. C.; Sheskey, P.; Marian, Q. et al. *Handbook of Pharmaceutical Excipients*, 6th ed.; Libros Digitales-Pharmaceutical Press: London, 2009.

(13) Guziewicz, N.; Best, A.; Perez-Ramirez, B.; et al. Lyophilized silk fibroin hydrogels for the sustained local delivery of therapeutic monoclonal antibodies. *Biomaterials* **2011**, *32*, 2642−2650.

(14) Wang, P.; Wang, Q.; Ren, T.; et al. Effects of Pluronic F127-PEG multi-gel-core on the release profile and pharmacodynamics of Exenatide loaded in PLGA microspheres. *Colloids Surf., B* **2016**, *147*, 360−367.

(15) Li, K.; Yu, L.; Liu, X.; et al. A long-acting formulation of a polypeptide drug exenatide in treatment of diabetes using an injectable block copolymer hydrogel. *Biomaterials* **2013**, *34*, 2834−2842.

(16) Qi, H.; Li, L.; Huang, C.; et al. Optimization and Physicochemical Characterization of Thermosensitive Poloxamer Gel Containing Puerarin for Ophthalmic Use. *Chem. Pharm. Bull.* **2006**, *54*, 1500−1507.

(17) Yu, M.; Yao, Q.; Zhang, Y.; et al. Core/shell PLGA microspheres with controllable in vivo release profile via rational core phase design. *Artif. Cells, Nanomed., Biotechnol.* **2018**, *46*, 1070−1079.

(18) Wang, P.; Zhou, X.; Chu, W.; et al. Exenatide-loaded microsphere/thermosensitive hydrogel long-acting delivery system with high drug bioactivity. *Int. J. Pharm.* **2017**, *528*, 62−75.

(19) Siepmann, J.; Elkharraz, K.; Siepmann, F.; et al. How autocatalysis accelerates drug release from PLGA-based microparticles: a quantitative treatment. *Biomacromolecules* **2005**, *6*, 2312−2319.

(20) Zolnik, B. S.; Burgess, D. J. Effect of acidic pH on PLGA microsphere degradation and release. *J. Controlled Release* **2007**, *122*, 338−344.

(21) Shenderova, A.; Burke, T. G.; Schwendeman, S. P. The acidic microclimate in poly(lactide-co-glycolide) microspheres stabilizes camptothecins. *Pharm. Res.* **1999**, *16*, 241−248.

(22) Li, S.; McCarthy, S. Further investigations on the hydrolytic degradation of poly (DL-lactide). *Biomaterials* **1999**, *20*, 35−44.

(23) Von Burkersroda, F.; Schedl, L.; Göpferich, A. Why degradable polymers undergo surface erosion or bulk erosion. *Biomaterials* **2002**, *23*, 4221−4231.

(24) Naghibzadeh, M.; Adabi, M.; Rahmani, H. R.; Mohsen, M.; Adabi, M. Evaluation of the effective forcespinning parameters controlling polyvinyl alcohol nanofibers diameter using artificial neural network. *Adv. Polym. Technol.* **2018**, *37*, 1608−1617.

(25) Kakade, S. M.; Hassan, D. H. Effects of Formulation Parameters on the Characteristics of Biodegradable Microspheres of Goserelin Acetate. *Asian J. Pharm.* **2018**, *12*, S691−S697.

(26) Lee, J.; Tan, C. Y.; Lee, S. K.; Kim, Y. H.; Lee, K. Y. Controlled delivery of heat shock protein using an injectable microsphere/hydrogel combination system for the treatment of myocardial infarction. *J. Controlled Release* **2009**, *137*, 196−202.

(27) Cui, F.; Cun, D.; Tao, A.; Yang, M.; Shi, K.; Zhao, M.; Guan, Y. Preparation and characterization of melittin-loaded poly (dl -lactic acid) or poly (dl -lactic-co-glycolic acid) microspheres made by the double emulsion method. *J. Controlled Release* **2005**, *107*, 310−319.

(28) Madani, F.; Esnaashari, S. S.; Mujokoro, B.; et al. Investigation of effective parameters on size of paclitaxel loaded PLGA nanoparticles. *Adv. Pharm. Bull.* **2018**, *8*, 77−84.

(29) Yang, Y.-Y.; Chung, T. S.; Ng, N. P. Morphology, drug distribution, and in vitro release profiles of biodegradable polymeric

microspheres containing protein fabricated by double-emulsion solvent extraction/evaporation method. *Biomaterials* **2001**, *22*, 231−241.

(30) Kilkenny, C.; Browne, W. J.; Cuthill, I.; et al. Animal Research: Reporting in vivo experiments: The ARRIVE guidelines. *J. Gene Med.* **2010**, *12*, 561−564.

(31) Zhang, S.; Han, J.; Leng, G.; et al. An LC−MS/MS method for the simultaneous determination of goserelin and testosterone in rat plasma for pharmacokinetic and pharmacodynamic studies. *J. Chromatogr. B: Anal. Technol. Biomed. Life Sci.* **2014**, *965*, 183−190.

(32) Ko, D. H.; Lee, K.; Jeon, S. H.; et al. Simultaneous Measurement of Serum Chemical Castration Agents and Testosterone Levels Using Ultra-Performance Liquid Chromatography−Tandem Mass Spectrometry. *J. Anal. Toxicol.* **2016**, *40*, 294−303.

(33) Pu, C.; Wang, Q.; Zhang, H.; et al. In Vitro-In Vivo Relationship of Amorphous Insoluble API (Progesterone) in PLGA Microspheres. *Pharm. Res.* **2017**, *34*, 2787−2797.

(34) Fu, X.; Ping, Q.; Gao, Y. Effects of formulation factors on encapsulation efficiency and release behaviour in vitro of huperzine A-PLGA microspheres. *J. Microencapsulation* **2005**, *22*, 57−66.

(35) Wu, H.; Wang, K.; Wang, H.; et al. Novel self-assembled tacrolimus nanoparticles cross-linking thermosensitive hydrogels for local rheumatoid arthritis therapy. *Colloids Surf., B* **2017**, *149*, 97−104.

(36) Malekpour, M. R.; Naghibzadeh, M.; Najafabadi, M. R. H.; Esnaashari, S. S.; et al. Effect of various parameters on encapsulation efficiency of mPEG-PLGA nanoparticles: artificial neural network. *Biointerface Res. Appl. Chem.* **2018**, *8*, 3267−3272.

(37) Shenderova, A.; Ding, A. G.; Schwendeman, S. P. Potentiometric Method for Determination of Microclimate pH in Poly(lactic-co-glycolic acid) Films. *Macromolecules* **2004**, *37*, 10052−10058.

(38) Gu, B.; Wang, Y.; Burgess, D. J. In vitro and in vivoperformance of dexamethasone loaded PLGA microspheres prepared using polymer blends. *Int. J. Pharm.* **2015**, *496*, 534−540.

(39) Kim, H. K.; Chung, H. J.; Park, T. G. Biodegradable polymeric microspheres with "open/closed" pores for sustained release of human growth hormone. *J. Controlled Release* **2006**, *112*, 167−174.

(40) Sun, Y.; W, J.; et al. Synchronic release of two hormonal contraceptives for about one month from the PLGA microspheres: in vitro and in vivo studies. *J. Controlled Release* **2008**, *129*, 192−199.

(41) Shah, S. S.; Cha, Y.; Pitt, C. G. Poly (glycolic acid-co- dl -lactic acid): diffusion or degradation controlled drug delivery? *J. Controlled Release* **1992**, *18*, 261−270.

(42) Bishara, A.; Domb, A. J. PLA stereocomplexes for controlled release of somatostatin analogue. *J. Controlled Release* **2005**, *107*, 474−483.

(43) Heya, T.; Okada, H.; Ogawa, Y.; Toguchi, H. In vitro and in vivo evaluation of thyrotrophin releasing hormone release from copoly(DL-lactic/glycolic acid) microspheres. *J. Pharm. Sci. A* **1994**, *83*, 636−640.

(44) Yang, Y. Y.; Chung, T. S.; et al. Morphology, drug distribution, and in vitro release profiles of biodegradable polymeric microspheres containing protein fabricated by double-emulsion solvent extraction/evaporation method. *Biomaterials* **2001**, *22*, 231−241.

(45) Mazzara, J. M.; Balagna, M. A.; et al. Healing kinetics of microneedle-formed pores in PLGA films. *J. Controlled Release* **2013**, *171*, 172−177.

(46) Cun, D.; Cui, F.; Yang, L.; Yang, M.; Yu, Y.; Yang, R. Characterization and release mechanism of melittin entrapped poly (lactic acid-co-glycolic acid) microspheres. *J. Drug Delivery Sci. Technol.* **2008**, *18*, 267−272.

(47) Zhang, H.; Pu, C.; et al. Physicochemical Characterization and Pharmacokinetics of Agomelatine-Loaded PLGA Microspheres for Intramuscular Injection. *Pharm. Res.* **2019**, *36*, No. 9.

(48) Jiang, G.; Thanoo, B. C.; Deluca, P. P. Effect of osmotic pressure in the solvent extraction phase on BSA release profile from PLGA microspheres. *Pharm. Dev. Technol.* **2002**, *7*, 391−399.

(49) Qi, F.; Wu, J.; Fan, Q.; He, F.; Tian, G.; Yang, T.; Ma, G.; Su, Z. Preparation of uniform-sized exenatide-loaded PLGA microspheres as long-effective release system with high encapsulation efficiency and bio-stability. *Colloids Surf., B* **2013**, *112*, 492−498.

(50) Stanković, M.; Tomar, J.; Hiemstra, C.; et al. Tailored protein release from biodegradable poly(ε-caprolactone-PEG)-b-poly(ε-caprolactone) multiblock-copolymer implants. *Eur. J. Pharm. Biopharm.* **2014**, *87*, 329−337.

(51) Kurian, L. A. Submonomer Synthesis and Structure-activity Relationship Studies of Azapeptide Inhibitors of the Insulin Receptor Tyrosine Kinase. PhD Dissertation; Seton Hall University, 2014.

(52) Walencik, P. K.; Kamila, S.-S.; Wieczorek, R.; et al. Impact of the Cu(II) ions on the chemical and biological properties of goserelin-coordination pattern, DNA degradation, oxidative reactivity and in vitro cytotoxicity. *J. Inorg. Biochem.* **2017**, *175*, 167−178.

(53) Asher, S. A.; Ludwig, M.; Johnson, C. R. ChemInform Abstract: UV Resonance Raman Excitation Profiles of the Aromatic Amino Acids. *Chem. Informationsdienst* **1986**, *17*, 3186−3197.

(54) Zhang, N.; Qiu, J.; Zheng, T.; et al. Goserelin promotes the apoptosis of epithelial ovarian cancer cells by upregulating forkhead box O1 through the PI3K/AKT signaling pathway. *Oncol. Rep.* **2018**, *39*, 1034−1042.

(55) Moore, H. C. F.; Unger, J. M.; et al. Goserelin for Ovarian Protection during Breast-Cancer Adjuvant Chemotherapy. *N. Engl. J. Med.* **2015**, *372*, 923−932.

(56) Wang, J.; Xu, B.; Yuan, P.; et al. Phase II Trial of Goserelin and Exemestane Combination Therapy in Premenopausal Women With Locally Advanced or Metastatic Breast Cancer. *Medicine* **2015**, *94*, No. e1006.

(57) Tomar, P.; Jain, N.; Agarwal, G. S.; et al. Goserelin loaded nanoparticles inhibit growth and induce apoptosis in human prostate cancer cell lines. *Drug Delivery Transl. Res.* **2012**, *2*, 265−271.

(58) Hutchinson, F. G. Continuous Release Pharmaceutical Compositions. U.S. Patent US5366734, 1994.

(59) Wei Sun, X. Z.; Wang, Tao. et al. Pharmaceutical Compositions of Goserelin Sustained Release Microspheres. U.S. Patent US20160022584, 2016.